



Bicarbonate secretion plays a role in chloride and water absorption of the European flounder intestine

M. Grosell, C. M. Wood, R. W. Wilson, N. R. Bury, C. Hogstrand, C. Rankin and F. B. Jensen

Am J Physiol Regul Integr Comp Physiol 288:936-946, 2005. First published Dec 2, 2004;
doi:10.1152/ajpregu.00684.2003

You might find this additional information useful...

This article cites 26 articles, 11 of which you can access free at:

<http://ajpregu.physiology.org/cgi/content/full/288/4/R936#BIBL>

Updated information and services including high-resolution figures, can be found at:

<http://ajpregu.physiology.org/cgi/content/full/288/4/R936>

Additional material and information about *American Journal of Physiology - Regulatory, Integrative and Comparative Physiology* can be found at:

<http://www.the-aps.org/publications/ajpregu>

This information is current as of January 11, 2006 .

Bicarbonate secretion plays a role in chloride and water absorption of the European flounder intestine

M. Grosell,¹ C. M. Wood,^{1,2} R. W. Wilson,³ N. R. Bury,⁴ C. Hogstrand,^{1,4} C. Rankin,⁵ and F. B. Jensen⁵

¹RSMAS, University of Miami, Miami, Florida; ²McMaster University, Hamilton, Ontario, Canada; ³Exeter University, Exeter; ⁴Kings College, London, United Kingdom; and ⁵University of Southern Denmark, Odense, Denmark

Submitted 1 December 2003; accepted in final form 1 December 2004

Grosell, M., C. M. Wood, R. W. Wilson, N. R. Bury, C. Hogstrand, C. Rankin, and F. B. Jensen. Bicarbonate secretion plays a role in chloride and water absorption of the European flounder intestine. *Am J Physiol Regul Integr Comp Physiol* 288: R936–R946, 2005. First published December 2, 2004; doi:10.1152/ajpregu.00684.2003.—Experiments performed on isolated intestinal segments from the marine teleost fish, the European flounder (*Platichthys flesus*), revealed that the intestinal epithelium is capable of secondary active HCO_3^- secretion in the order of $0.2\text{--}0.3\ \mu\text{mol}\cdot\text{cm}^{-2}\cdot\text{h}^{-1}$ against an apparent electrochemical gradient. The HCO_3^- secretion occurs via anion exchange, is dependent on mucosal Cl^- , results in very high mucosal HCO_3^- concentrations, and contributes significantly to Cl^- and fluid absorption. This present study was conducted under in vivo-like conditions, with mucosal saline resembling intestinal fluids in vivo. These conditions result in a transepithelial potential of $-16.2\ \text{mV}$ (serosal side negative), which is very different from the $-2.2\ \text{mV}$ observed under symmetrical conditions. Under these conditions, we found a significant part of the HCO_3^- secretion is fueled by endogenous epithelial CO_2 hydration mediated by carbonic anhydrase because acetazolamide ($10^{-4}\ \text{M}$) was found to inhibit HCO_3^- secretion and removal of serosal CO_2 was found not to influence HCO_3^- secretion. Reversal of the epithelial electrochemical gradient for Cl^- (removal of serosal Cl^-) and elevation of serosal HCO_3^- resulted in enhanced HCO_3^- secretion and enhanced Cl^- and fluid absorption. Cl^- absorption via an anion exchange system appears to partly drive fluid absorption across the intestine in the absence of net Na^+ absorption.

HCO_3^- secretion; chloride absorption; carbonic anhydrase; osmoregulation; marine teleost

IT IS WELL ESTABLISHED THAT marine teleosts drink seawater and that the intestine has a vital role in osmoregulation by performing water absorption (18, 24, 25) necessary to compensate for the continuous osmotic water loss to the marine environment. This water absorption is generally accepted to be coupled to Na^+ and Cl^- absorption driven by $\text{Na}^+\text{--Cl}^-$ and $\text{Na}^+\text{--K}^+\text{--}2\text{Cl}^-$ cotransporters (15, 18), but an additional, perhaps major contribution to Cl^- uptake and thereby fluid absorption by anion exchange has so far largely been ignored.

High HCO_3^- concentrations in the intestinal fluids of marine teleost fish were first suggested by Shehadeh and Gordon (24) more than three decades ago and subsequently documented for the first time by Walsh et al. (26) more than 10 yr ago. Only recently, however, has this unique phenomenon been investigated in greater detail (7, 8, 9, 10, 28–31). $\text{Cl}^-/\text{HCO}_3^-$ exchange across the apical membrane of the marine teleost intestine is responsible for the extremely high HCO_3^- concentrations found in the intestinal lumen (8, 10, 28, 30, 31). It can

result in HCO_3^- concentrations in excess of 100 mM, which is much higher than the 5–10 mM found in the extracellular fluids of these water-breathing vertebrates. This substantial chemical gradient and the low blood side negative transepithelial potential (TEP) of marine teleost intestinal epithelia (18) strongly suggest active bicarbonate secretion, but this remains to be documented.

Active HCO_3^- secretion is perhaps best known to occur from the exocrine pancreatic ducts, which can secrete fluid containing HCO_3^- concentrations up to 140 mM (22), i.e., concentrations very similar to those found in the marine teleost intestine. Pancreatic exocrine HCO_3^- secretion serves digestion; however, this is clearly not the case for the marine teleost intestine (28, 30, 31). Rather, in these marine animals, HCO_3^- secretion is perhaps involved in osmoregulation by reducing the osmolality of the intestinal fluids by cation-carbonate precipitation, thereby aiding fluid absorption indirectly and by contributing to Cl^- and perhaps fluid absorption directly through the anion exchange process (31). Marine fish live in a hypercalcemic environment, so the precipitation (and subsequent rectal excretion) of imbibed calcium as insoluble carbonates also minimizes the intestinal absorption of excess calcium, indicating a further role for HCO_3^- secretion in calcium homeostasis (31).

Fluid absorption linked to NaCl absorption via $\text{Na}^+\text{--Cl}^-$ and $\text{Na}^+\text{--K}^+\text{--}2\text{Cl}^-$ cotransporters relies on the electrochemical gradient for Na^+ , which in turn is generated by the basolateral electrogenic $\text{Na}^+\text{--K}^+\text{--ATPase}$. Although this mechanism accounts for part of the intestinal Cl^- absorption, simultaneous measurements of net Na^+ and Cl^- absorption on several species of marine teleost fish have revealed that Cl^- absorption rates in all cases greatly exceed the corresponding rates for Na^+ (5, 7, 8, 10, 19, 20). The stoichiometry of $\text{Na}^+\text{--K}^+\text{--}2\text{Cl}^-$ cotransporters can contribute to Cl^- absorption exceeding Na^+ absorption, with K^+ absorption making up for any $\text{Na}^+\text{--Cl}^-$ gap. However, it is likely that $\text{Cl}^-/\text{HCO}_3^-$ exchange also contributes to the higher Cl^- absorption rates: net HCO_3^- secretion rates, when measured (7, 8, 10), were similar in magnitude to the gap between net Na^+ and net Cl^- absorption rates (5, 7, 8, 10, 19, 20).

In the present study performed on the European flounder, *Platichthys flesus*, one objective was to determine whether the intestinal epithelium is capable of performing truly active HCO_3^- transport. This objective was pursued by measuring both HCO_3^- transport rates and TEP across isolated intestinal segments at a range of transepithelial HCO_3^- gradients. The Cl^- dependence of intestinal HCO_3^- secretion was tested by experiments with Cl^- -free solutions on the luminal and the

Address for reprint requests and other correspondence: M. Grosell, RSMAS, Division of Marine Biology and Fisheries, Univ. of Miami, 4600 Rickenbacker Causeway, Miami, FL 33149-1098 (E-mail: mgrosell@rsmas.miami.edu).

The costs of publication of this article were defrayed in part by the payment of page charges. The article must therefore be hereby marked “advertisement” in accordance with 18 U.S.C. Section 1734 solely to indicate this fact.

serosal side of the epithelium. An additional objective was to determine whether HCO_3^- secretion via anion exchange contributes significantly to Cl^- and thus water absorption. Experiments employing acetazoamide, a carbonic anhydrase inhibitor, were designed to test the hypothesis of involvement of carbonic anhydrase in HCO_3^- secretion and to potentially inhibit HCO_3^- secretion. Attempts to inhibit and stimulate intestinal HCO_3^- secretion to test the potential contribution to Cl^- absorption also included experiments with reduced and elevated serosal CO_2 levels. These experiments also served to address the question regarding the source for intestinal HCO_3^- secretion. Our hypothesis was that reduced serosal CO_2 might result in reduced HCO_3^- secretion if the normal origin was serosal rather than endogenous, due to substrate depletion, and that this in turn might reduce Cl^- and fluid absorption. Conversely, elevated serosal CO_2 was hypothesized to stimulate intestinal HCO_3^- secretion and thereby Cl^- and fluid absorption.

MATERIALS AND METHODS

Experimental animals. European flounder, *Platichthys flesus*, were obtained by local fisherman from inshore areas of variable salinity and acclimated to laboratory holding conditions at a salinity of 20‰ for a minimum of 5 days at the marine station in Kerteminde, Fyn, Denmark. Fish were then transferred to 33‰ salinity water (full-strength seawater) and were allowed to acclimate for an additional 3 days before experimentation. Fish were not fed during holding and acclimation, and experimental temperature was kept constant at 12°C via climate-controlled laboratory facilities.

General experimental approach. Fish were killed by an overdose of tricaine methanesulfonate (MS-222; 0.25 g/l), and the entire intestine was obtained by dissection. The intestine was separated from the stomach just posterior to the pyloric sphincter. Care was taken not to include the distal part of the gastrointestinal tract (the rectum), which is separated from the posterior intestine by a distinct sphincter. A short length of heat-flared polyethylene (PE) tubing was tied in the anterior end of the intestine, and the entire intestine was flushed with 20 ml of the appropriate mucosal saline (see Table 1). Subsequently, sacs were prepared from the anterior, the mid-, and the posterior segments of the intestine, each ~30 mm in length. Each segment was fitted with a PE-tubing catheter (PE-60) tied in the proximal end with double silk ligatures and closed in the distal end again with double silk ligatures. The catheter served to fill and drain the sac preparation. The sacs were

filled with the relevant mucosal saline, and a representative sample (300 μl) was obtained as follows. After the sac was moderately overfilled, saline was drawn from the sac preparation through the PE catheter into a syringe and flushed back and forth several times to ensure complete mixing before the final sample was taken. The catheter was thereafter sealed, and the sac preparation was blotted dry with paper towels. The mass of the preparation (consisting of intestinal tissue and mucosal saline) was determined to the nearest 100 μg . Subsequently, the sac preparation was placed in a fixed volume (15 ml) of the relevant serosal saline (see Table 1 for details), which was preequilibrated for a minimum of 30 min and continuously gassed during experiments through a gas diffuser with 0.5% CO_2 and 99.5% O_2 from a Wösthoff 301 (Bochum, Germany) Digamix 2M301/a-F gas-mixing pump, unless otherwise stated. Saline composition was chosen partly from a previous study (9) and partly from measurements performed on plasma and intestinal fluid composition in fish from the same batch as fish used for the sac experiments (data not shown).

An initial sample of serosal saline (1 ml) was obtained at the start of the flux period, which ranged from 2 to 4 h depending on the type of experiment. At the end of the flux period (exact time noted), another sample of the serosal saline (1 ml) was obtained, and the sac preparation was removed from the flux chamber, blotted dry as above, and reweighed. After the masses of the sac preparation and the contained mucosal saline were measured, we obtained a sample of the mucosal saline via the filling catheter. In some cases, the sac preparation was then refilled with the appropriate mucosal saline and the serosal saline was replaced before initiation of subsequent flux measurements. After the final flux period (never more than three flux periods), the sac preparation was drained completely, cut open by a longitudinal incision, and thoroughly blotted dry on both the inside and outside, after which the mass of the intestinal tissue (including catheter) was determined. The preparation was stored at 4°C overnight in zip-lock bags to ensure complete muscle relaxation before we determined the gross surface area of the exposed intestinal tissue by tracing its outline onto graph paper. We used this gross surface area to normalize measured ion and water flux values.

With the exception of experiments designed for measurement of TEP outlined below, all mucosal salines were labeled with ^{22}Na and ^{36}Cl (Amersham, 0.05–0.2 and 0.3 $\mu\text{Ci/ml}$, respectively) to allow for measurements of unidirectional fluxes of these ions as outlined previously (8).

Viability of the preparation. To ensure that the viability of the preparation was sufficient to perform several subsequent flux measurements, we first performed a time series experiment. We prepared segments from all three regions of the intestine as outlined above using an HCO_3^- concentration of 11 mM in both the mucosal and the serosal saline. Three subsequent 2-h flux measurements were conducted with exchange of mucosal and serosal saline between flux periods. These experiments also allowed for comparison of transport rates in sac preparations made from the anterior, mid-, and posterior segments of the intestine.

HCO_3^- secretion against an electrochemical gradient. To examine whether intestinal HCO_3^- secretion occurred against an electrochemical gradient, HCO_3^- secretion was measured under varying transepithelial HCO_3^- gradients. This was done by measuring HCO_3^- secretion in preparations with 1, 11, and 25 mM HCO_3^- in the mucosal saline while serosal saline was kept constant at 11 mM (using 3 intestinal segments from each of 4 fish) and by varying serosal saline HCO_3^- concentrations between 1, 11, and 25 mM while keeping the mucosal saline constant at 11 mM (3 intestinal segments from each of 4 fish).

HCO_3^- concentrations in the mucosal saline were adjusted by changing the amount of choline- HCO_3 to yield 1, 11, and 25 mM. Low serosal HCO_3^- was achieved by replacing 10 of the 11 mM NaHCO_3 with 10 mM sodium gluconate, and the intermediate and high serosal HCO_3^- levels were achieved by addition of 10 and 24 mM choline- HCO_3 , respectively. We exploited the longevity of the prep-

Table 1. General saline composition

	Mucosal Saline		Serosal Saline	
	Control	Cl^- free	Control	Cl^- free
$\text{CaCl}_2(2\text{H}_2\text{O})$	5.0		3.0	
Calcium gluconate		5.0		3.0
Glucose			5.55	5.55
KCl	5.0		2.5	
Potassium gluconate		5.0		2.5
$\text{MgCl}_2(7\text{H}_2\text{O})$	22.5			
MgSO_4	77.5	100.0	1.5	1.5
NaCl	49.0		131.0	
Sodium gluconate		49.0		131.0
NaHCO_3	1.0	1.0	11.0	11.0
$\text{NaH}_2\text{PO}_4(\text{H}_2\text{O})$			2.97	2.97
Choline- HCO_3	10.0	10.0		
pH*	8.0	8.0	7.9	7.9
Osmolality†	308	308	308	308

All values are in mM, except osmolality (mosmol/kg H_2O) and pH. *When gassed with 0.5% CO_2 in O_2 ; †adjusted with mannitol.

ation by performing three subsequent measurements on each sac preparation, randomizing the order of mucosal and serosal HCO_3^- concentrations (3 intestinal segments from each of 4 fish). In all cases, salines were osmotically compensated with mannitol to ensure the same osmolality of mucosal and serosal salines regardless of HCO_3^- concentrations.

TEP measurements were performed under the above conditions on sac preparations of all three segments from a total of three individual fish. The TEP was measured under traditional symmetrical conditions with serosal saline (which resembled the blood plasma composition; see Table 1) on both surfaces and also with mucosal saline (which approached the *in vivo* intestinal fluid composition; see Table 1) on the mucosal surface and serosal saline on the serosal surface. Under the latter condition, HCO_3^- concentrations were manipulated. As above, the order of experimental conditions was randomized throughout. We performed TEP measurements using agar/salt bridges (3 M KCl in 4% agar) connected through Ag/AgCl electrodes (World Precision Instruments) to a Radiometer (Copenhagen, Denmark) PHM 84 high-impedance electrometer. We expressed all TEP values using a mucosal reference of 0 mV; the sac preparation was exposed to mucosal and serosal salines of appropriate composition. Because the Cl^- concentration differed between the serosal and the mucosal medium (in some cases), electrode tip potential (routinely <1 mV) was recorded, and TEP measurements were corrected accordingly. Triplicate measurements (after stabilization) over a 5-min period were averaged in all cases.

Source of HCO_3^- . After we established that intestinal HCO_3^- secretion occurred against an apparent gradient, the source of HCO_3^- (i.e., originating from either endogenous CO_2 generation or serosal CO_2) was considered. In these experiments, performed on all three intestinal segments from a total of six fish, the serosal saline was gassed with pure O_2 , 0.5% CO_2 in O_2 , or 2% CO_2 in O_2 to assess the potential contribution of serosal CO_2 . Both serosal and mucosal salines (containing 11 mM HCO_3^-) were preequilibrated with these gases before the 3-h flux period, and appropriate gassing of serosal salines was continued throughout the experiment.

Dependence on carbonic anhydrase. Observations of stimulated HCO_3^- secretion in the presence of elevated serosal CO_2 led to the hypothesis of involvement of carbonic anhydrase. To test whether carbonic anhydrase may fuel HCO_3^- secretion by facilitating CO_2 hydration, the carbonic anhydrase inhibitor acetazolamide was employed. To ensure maximal effect, acetazolamide was injected into the caudal artery of experimental fish ($n = 6$) 12 h before experimentation to yield approximately 10^{-4} M acetazolamide in the extracellular fluids, whereas control fish ($n = 6$) were sham injected (see below). Four-hour fluxes with acetazolamide (10^{-4} M), which was present in both mucosal and serosal saline (both containing 11 mM HCO_3^-), were performed on all three intestinal segments. Acetazolamide was first dissolved in 0.2 M NaOH and titrated down to pH 7.9 with 0.2 M HCl and then diluted with double-distilled water to yield 140 mM NaCl. This cocktail was used for injection, and an identical fresh batch was used to spike the serosal and mucosal salines for the sac preparation experiments. An injection cocktail lacking acetazolamide was used for the control fish. No apparent effects of acetazolamide and sham injections were observed on fish before dissection.

Dependence on chloride. To test the importance of Cl^- for the intestinal HCO_3^- secretion process, dependencies on both mucosal and serosal Cl^- were evaluated. Again exploiting the longevity of the preparation's viability, we performed three subsequent flux measurements on sac preparations from all segments of the intestine (see figure legends for n numbers). At the end of each flux period, the mucosal saline was replaced after thorough rinsing (consisting of three refillings), and the serosal saline was renewed. Control experiments with preparations bathed in standard mucosal and serosal saline were performed, together with experiments employing Cl^- -free serosal and mucosal salines, again in random order. For these experiments, Cl^- salts were replaced with appropriate gluconate salts (see Table 1

for details). TEP was also measured under these conditions, as outlined above, using a separate set of preparations ($n = 5$ fish).

Analytic techniques and calculations. Mucosal (50 μl) and serosal (500 μl) saline samples from the beginning and end of each flux period were prepared for measurements of γ -radioactivity from ^{22}Na on a gamma counter (1480 Wizard 3 automatic, Wallac, Turku, Finland). We also measured total β -radioactivity from ^{36}Cl and ^{22}Na in the initial and final saline samples (volumes as above) using a scintillation counter (Packard 2200 CA Tri-carb, Packard, Groningen, Netherlands). Samples were prepared for scintillation counting by addition of 10 ml of scintillation fluid. Mucosal samples were spiked with 450 μl of nonradioactive saline, resulting in the same volume and sample-to-scintillation fluid ratio in serosal and mucosal samples. The two counters were cross-calibrated for ^{22}Na radioactivity detection efficiency, and the contribution of ^{22}Na to the total β -radioactivity was subtracted from the total β -radioactivity to determine the ^{36}Cl β -radioactivity.

Na^+ and Cl^- concentrations in mucosal and serosal salines were measured by atomic absorption spectroscopy after appropriate dilutions (Varian, SpectraAA220FS) and by a Radiometer CMT10 chloridometer, respectively. Osmolality was measured with Gonotec Osmomat 030.

We measured serosal and mucosal saline pH using Radiometer microelectrodes (BMS3 system), with the signal displayed on a PHM 73 blood-gas monitor. We measured total CO_2 in all salines using a CO_2 analyzer (Mettler Toledo 965). The concentration of HCO_3^- equivalents was calculated from these measurements according to the Henderson-Hasselbalch equation. Initially, HCO_3^- concentrations were determined from measurements of total CO_2 and pH using the following rearrangement of the Henderson-Hasselbalch equation:

$$[\text{HCO}_3^-] = [\text{total CO}_2] / (1 + 10^{\text{pH} - \text{pK}_1})$$

where brackets indicate concentration and where pK_1 is the appropriate ionic strength (1/3 seawater), obtained from Ref. 27. Subsequently, the contribution of molecular CO_2 was determined as

$$[\text{Molecular CO}_2] = [\text{HCO}_3^-] / (1 + 10^{\text{pH} - \text{pK}_1})$$

using the apparent pK_1 for ionic strength equivalent of teleost plasma at 12°C for the measured pH from Boutilier et al. (3).

Thus $[\text{total CO}_2] = [\text{molecular CO}_2] + [\text{HCO}_3^-] + [\text{CO}_3^{2-}]$. In practice the molecular CO_2 is generally very low ($<10^{-9}$ M) at the pH values used in the present experiments; thus

$$[\text{CO}_3^{2-}] = [\text{total CO}_2] - [\text{HCO}_3^-]$$

From the estimated concentrations of HCO_3^- and CO_3^{2-} , we determined the total HCO_3^- equivalents present in a saline sample as $[\text{HCO}_3^-] + 2[\text{CO}_3^{2-}]$.

The validity of this approach has been established previously (7), which showed a correlation coefficient (r^2) of 0.999 between HCO_3^- equivalents determined as described above from measurements of pH and total CO_2 and HCO_3^- determined by double-endpoint titration (titratable alkalinity). For simplicity, hereafter in the text "concentration of HCO_3^- equivalents" is referred to as " HCO_3^- concentrations."

The internal mucosal saline volumes of each individual sac preparation at the beginning and end of the experiments were determined by subtracting the mass of the empty sac preparation from the corresponding initial or final total mass of the filled preparation. Net fluid transport was determined from the difference in total mass over the experimental period, taking into account the gross surface area of exposed epithelium and time elapsed. Net fluxes of Na^+ , Cl^- , and HCO_3^- were calculated from the differences in mucosal saline volume and ion concentration at the beginning and end of each flux period, again taking into account the gross surface area and time elapsed.

Unidirectional mucosal-to-serosal Cl^- transport was calculated from the appearance of the ^{36}Cl isotope in the serosal saline, and unidirectional Na^+ transport was calculated from the disappearance of

^{22}Na from the mucosal saline. For both ions, the mean of the corresponding specific activities in the mucosal saline at the start and the end of the flux period allowed for calculation of absolute ion flux rates. Unidirectional serosal-to-mucosal Na^+ and Cl^- transports were determined from the individual differences between the corresponding net flux and unidirectional mucosal-to-serosal flux rate.

Statistical evaluation and data presentation. Data are presented as absolute values, expressed as means \pm SE of n (number of samples). Means were compared by the use of paired or unpaired Student's t -test, depending on experimental design. Subsequent measurements on the same preparation were compared with the paired Student's t -test. Whenever appropriate, the Bonferroni multisample comparison correction was employed. In all cases, means were considered significantly different at $P < 0.05$.

Mucosal-to-serosal transport is considered absorption and indicated as positive values throughout, and serosal-to-mucosal transport is considered secretion and is indicated as negative values throughout.

RESULTS

Preparation viability and regional differences. Based on constant net flux of HCO_3^- , Na^+ , and Cl^- as well as unidirectional Na^+ and Cl^- flux rates over three subsequent 2-h flux periods, the intestinal preparations appeared viable and stable at least 6 h after initial preparation (Table 2). In agreement with previous reports (7, 8, 10), there were no significant differences in net ion transport, unidirectional Na^+ and Cl^- flux rates, or fluid absorption rates among the three intestinal segments used in the present study (Table 3). Combining measurements from control preparations in all experiments further supported this observation (data not shown), with overall mean values being $-0.28 \pm 0.02 \mu\text{mol}\cdot\text{cm}^{-2}\cdot\text{h}^{-1}$ for net HCO_3^- secretion, $2.12 \pm 0.30 \mu\text{l}\cdot\text{cm}^{-2}\cdot\text{h}^{-1}$ for fluid absorption, and $0.58 \pm 0.04 \mu\text{mol}\cdot\text{cm}^{-2}\cdot\text{h}^{-1}$ for net Cl^- absorption ($n = 99$). Unexpectedly, net Na^+ transport was characterized by secretion in the order of $-0.37 \pm 0.04 \mu\text{mol}\cdot\text{cm}^{-2}\cdot\text{h}^{-1}$. Because of the homogeneity among intestinal segments, data obtained from the anterior, mid-, and posterior segments were combined and presented as one in Figs. 1–7.

Effects of HCO_3^- gradients. Intestinal HCO_3^- secretion was stimulated by elevated serosal HCO_3^- concentrations (Fig. 1). Net Cl^- absorption and fluid movement tended to be higher with higher serosal HCO_3^- and thus HCO_3^- secretion rates. Interestingly, HCO_3^- secretion was present even with a serosal HCO_3^- concentration as low as 1 mM and with a mucosal HCO_3^- concentration of 11 mM at the beginning of the flux period (Fig. 1A). Conversely, elevated mucosal HCO_3^- concentrations reduced intestinal net HCO_3^- secretion in the presence of 11 mM serosal HCO_3^- , whereas low mucosal HCO_3^- concentrations resulted in highly elevated HCO_3^- secretion (Fig. 2).

When the preparations were exposed to serosal saline (which duplicated blood plasma composition) on both sides (symmetrical conditions), TEP was only -2.2 ± 0.6 mV. However, when the preparations were exposed to in vivo-like conditions (mucosal saline in the lumen, Table 1), the TEP decreased markedly to -16.2 ± 2.3 mV. Varying the transepithelial HCO_3^- gradient under in vivo-like conditions did not significantly influence TEP (Fig. 3).

Influence of extracellular CO_2 . Changing the gasing of serosal saline from 0.5% CO_2 -99.5% O_2 to 0% CO_2 -100% O_2 did not influence HCO_3^- secretion, unidirectional and net fluxes of Na^+ and Cl^- , or fluid absorption (Fig. 4). Elevating CO_2 to 2%, however, approximately doubled HCO_3^- secretion rates and elevated net Cl^- and fluid absorption. In addition, the net Na^+ loss seen under control conditions was reduced (Fig. 4).

Effects of acetazolamide. The carbonic anhydrase inhibitor acetazolamide when applied at 10^{-4} M reduced intestinal HCO_3^- secretion by 30–40% but did not influence any of the other measured intestinal transport parameters (Fig. 5).

Dependence on Cl^- . Intestinal HCO_3^- secretion in the European flounder was clearly dependent on mucosal Cl^- , since removal of luminal Cl^- reduced HCO_3^- secretion by more than 50%. In addition, net Na^+ loss was greatly enhanced, net Cl^- flux shifted to efflux, and fluid absorption was greatly impaired in the absence of mucosal Cl^- (Fig. 6). Luminal Cl^- removal furthermore resulted in a significantly less negative TEP (Fig. 7). Removal of serosal Cl^- enhanced net Cl^- absorption and stimulated HCO_3^- secretion and net Na^+ as well as fluid absorption (Fig. 6). In contrast to mucosal Cl^- removal, serosal Cl^- removal resulted in a significantly more negative TEP (Fig. 7). In addition, this series of TEP measurements (Fig. 7) confirmed the pattern of Fig. 5, showing that placement of serosal saline on both surfaces (symmetrical conditions) resulted in a small near-zero TEP, whereas establishment of normal in vivo-like conditions with the appropriate mucosal and serosal saline composition resulted in a much more negative TEP.

DISCUSSION

Active HCO_3^- secretion? In isolated flounder intestinal segments, HCO_3^- secretion occurs against a chemical gradient, with a TEP of -16.2 mV serosal side negative. The recorded TEP under in vivo-like conditions was much higher than the corresponding value obtained under symmetrical conditions (serosal saline on both sides of the epithelium). This is consistent with previous reports for intestinal preparations of the European flounder (30) and the winter flounder, *Pseudopleuronectes americanus* (12), and the gall bladder epithelium of

Table 2. Ion flux rates during three consecutive flux periods

Time, h	Ion Transport Rate, $\mu\text{mol}\cdot\text{cm}^{-2}\cdot\text{h}^{-1}$						
	HCO_3^- net flux	Cl^- net flux	Cl^- influx	Cl^- efflux	Na^+ net flux	Na^+ influx	Na^+ efflux
0–2	-0.44 ± 0.06	0.24 ± 0.31	3.13 ± 0.47	-2.90 ± 0.49	-0.40 ± 0.20	1.57 ± 0.39	-1.97 ± 0.27
2–4	-0.26 ± 0.03	0.08 ± 0.36	2.10 ± 0.33	-2.02 ± 0.54	-0.56 ± 0.18	1.76 ± 0.25	-2.31 ± 0.26
4–6	-0.33 ± 0.06	0.68 ± 0.27	2.83 ± 0.46	-2.15 ± 0.48	-0.44 ± 0.21	2.40 ± 0.47	-2.84 ± 0.42

Values are means \pm SE; $n = 15, 18$, and 11 samples for the 0–2, 2–4, and 4–6 h flux periods, respectively. Net flux of HCO_3^- (negative to indicate secretion), net flux and influx rates, and efflux rates of Cl^- and Na^+ in isolated intestinal segments from the European flounder during 3 subsequent 2-h flux period are shown. There were no significant differences across time ($P < 0.05$).

Table 3. Ion and water flux rates in three intestinal segments

Segment	Ion and Water Transport Rate, $\mu\text{mol}\cdot\text{cm}^{-2}\cdot\text{h}^{-1}$							Water Transport Rate (H_2O net flux), $\mu\text{l}\cdot\text{cm}^{-2}\cdot\text{h}^{-1}$
	HCO_3^- net flux	Cl^- net flux	Cl^- influx	Cl^- efflux	Na^+ net flux	Na^+ influx	Na^+ efflux	
Ant	-0.27 ± 0.05	-0.30 ± 0.32	3.28 ± 0.51	-3.58 ± 0.55	-0.68 ± 0.16	1.34 ± 0.22	-2.02 ± 0.24	1.69 ± 0.93
Mid	-0.33 ± 0.04	0.44 ± 0.40	2.40 ± 0.40	-1.96 ± 0.55	-0.53 ± 0.23	2.01 ± 0.35	-2.54 ± 0.34	1.80 ± 1.49
Post	-0.44 ± 0.06	0.67 ± 0.24	2.27 ± 0.33	-1.60 ± 0.32	-0.22 ± 0.18	2.17 ± 0.44	-2.40 ± 0.34	1.65 ± 1.74

Values are means \pm SE; $n = 15$ measurements in all cases. Net flux of HCO_3^- (negative to indicate secretion), net flux and influx rates, and efflux rates of Cl^- and Na^+ as well as net fluid movement in isolated intestinal segments of the anterior (Ant), mid-, and posterior (Post) regions of the intestine from the European flounder are shown. There were no significant differences among regions ($P < 0.05$).

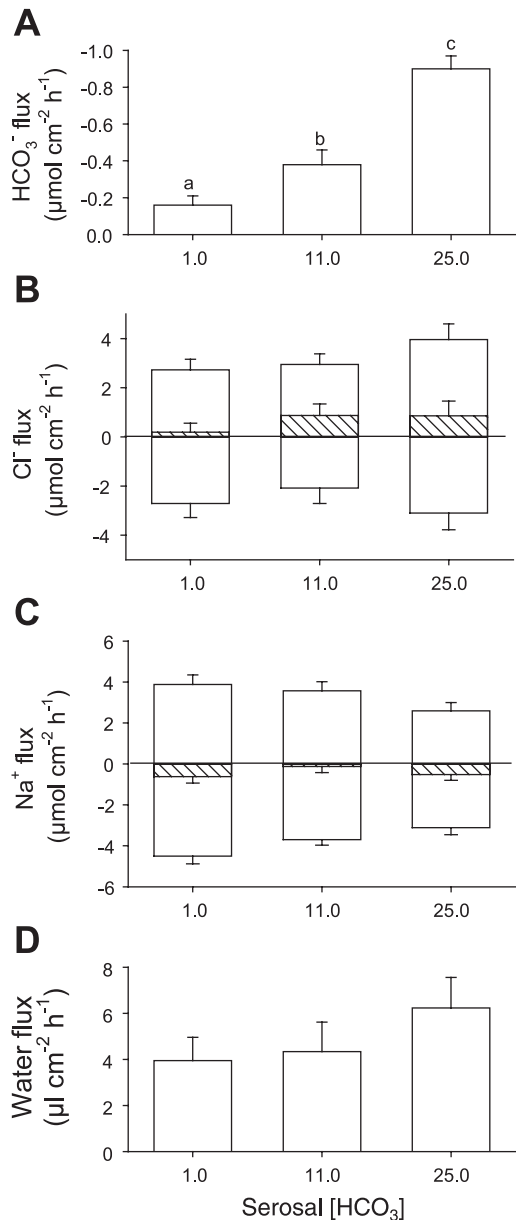


Fig. 1. Net flux of HCO_3^- (A), unidirectional efflux and influx rates (open bars) and net flux rates (hatched bars) of Cl^- (B) and Na^+ (C), and net water movement (D) in isolated intestinal segments from the European flounder at different serosal HCO_3^- concentrations ($[\text{HCO}_3^-]$). Mucosal $[\text{HCO}_3^-]$ was 11 mM. Results are means \pm SE; $n = 12$ measurements in all cases. Means labeled with different letters are significantly different ($P < 0.05$).

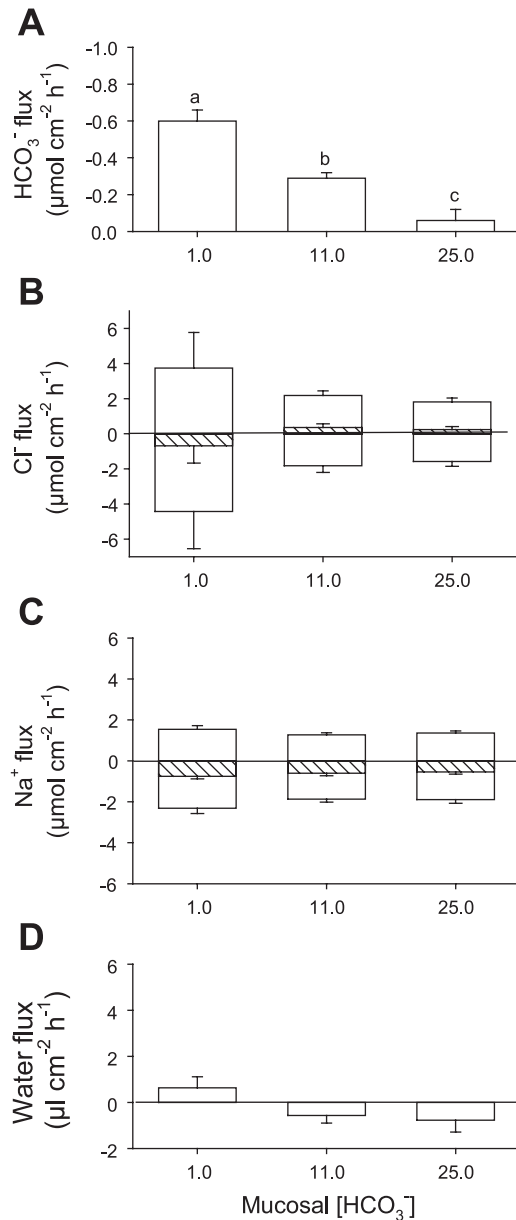


Fig. 2. Net flux of HCO_3^- (A), unidirectional efflux and influx rates (open bars) and net flux rates (hatched bars) of Cl^- (B) and Na^+ (C), and net water movement (D) in isolated intestinal segments from the European flounder at different mucosal $[\text{HCO}_3^-]$. Serosal $[\text{HCO}_3^-]$ was 11 mM. Results are means \pm SE; $n = 12$ measurements in all cases. Means labeled with different letters are significantly different ($P < 0.05$).

Intestinal transepithelial potential (TEP)

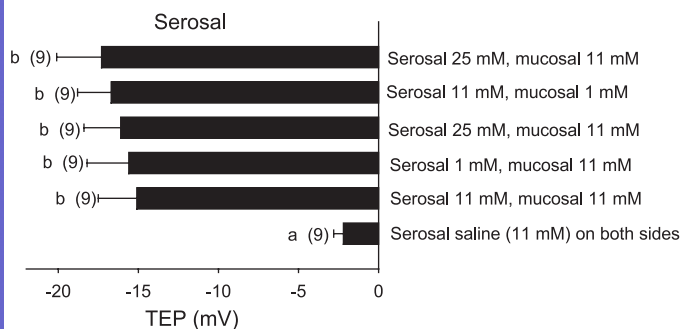


Fig. 3. Transepithelial potential (TEP) across the intestinal epithelia of the European flounder under symmetrical (serosal saline on both sides) and asymmetrical conditions (mucosal saline on luminal side, serosal saline on basolateral side) in vitro, with different mucosal and serosal HCO_3^- . Results are means \pm SE; n (no. of measurements) are given in parentheses. Means labeled with different letters are statistically significantly different ($P < 0.05$).

the rainbow trout, *Oncorhynchus mykiss* (11). Although the type of mucosal saline influences TEP, varying the HCO_3^- gradient did not appear to have an effect (Fig. 5). The pH varied with HCO_3^- concentration, but even the combined effect of altering pH and HCO_3^- concentration did not significantly alter TEP. The Nernst equation provides the equilibrium potential (E) required to sustain a given chemical gradient across an epithelium: $E = [(RT)/(zF)]2.303 \times \{\log ([X_o]/[X_i])\}$, where X represents the ion in question on the outer (o) and inner (i) side of the epithelium, z is the valence of this ion, and R , T , and F have their usual meanings. When isolated segments were bathed in 1 mM HCO_3^- in the serosal saline and in 11 mM in the mucosal saline (Fig. 1), the epithelial potential required, according to the Nernst equation, for continuous secretion of HCO_3^- would have to be lower than -58.9 mV serosal side negative for nonactive transport to occur. This predicted equilibrium potential is much more negative than the recorded TEP under those conditions (Fig. 3), demonstrating that the intestinal epithelium is capable of performing (secondary) active HCO_3^- secretion as hypothesized. Because HCO_3^- secretion occurs via apical anion exchange (see below), which is not in itself ATP consuming, this secretion must be of secondary active nature. Varying the mucosal HCO_3^- concentration revealed that, although HCO_3^- secretion can occur against an electrochemical gradient, it is almost completely abolished when mucosal HCO_3^- concentrations are elevated to 25 mM (Fig. 2).

Considering individual HCO_3^- secretion rates, measured in the HCO_3^- gradient experiments, as a function of the corresponding mean HCO_3^- gradient across the epithelium, it appears that transepithelial HCO_3^- secretion can occur against an absolute gradient of up to 17 mM (Fig. 8A). This apparent limitation compared with in vivo gradients (luminal concentrations up to 100 mM) is consistent with previous reports of lower HCO_3^- secretion rates in isolated epithelia than those seen in intact animals (31). Because the isolated intestinal preparation appears stable and healthy for the duration of these experiments, this may suggest that the HCO_3^- secretory process is not fully stimulated or activated in these preparations. Nevertheless, the isolated intestinal segments are clearly capable of active HCO_3^- secretion even in this nonstimulated state. This becomes clear when considering individual HCO_3^- secretion rates now as a function of transepithelial HCO_3^- concen-

tration ratio, which is thermodynamically relevant (see the Nernst equation), rather than absolute concentration differences. HCO_3^- secretion in the intestinal sac preparations continued until $\log (\text{serosal } [\text{HCO}_3^-]/\text{mucosal } [\text{HCO}_3^-])$ became as low as -1.7 (Fig. 8B), which corresponds to an equilibrium potential of -96 mV, clearly much more negative than the TEP measured under the same conditions (Fig. 3).

Source of HCO_3^- . The experiments with elevated and reduced serosal HCO_3^- concentrations (Fig. 1) suggest that serosal HCO_3^- may provide substrate for intestinal HCO_3^- secretion. HCO_3^- could enter the intestinal epithelial cells across the basolateral $\text{Cl}^-/\text{HCO}_3^-$ exchanger (AE) as first proposed by

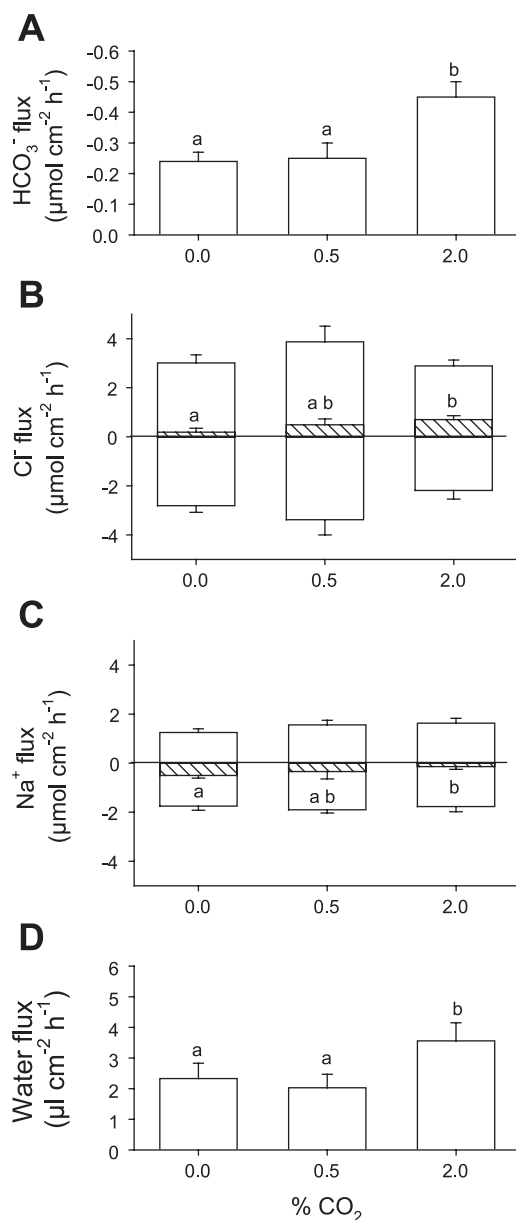


Fig. 4. Net flux of HCO_3^- (A), unidirectional efflux and influx rates (open bars) and net flux rates (hatched bars) of Cl^- (B) and Na^+ (C), and net water movement (D) in isolated intestinal segments from the European flounder bathed in solution gassed with 0, 0.5, and 2.0% CO_2 in O_2 . Results are means \pm SE; $n = 9, 15$, and 9 measurements for 0, 0.5, and 2.0% CO_2 , respectively. Means labeled with different letters are significantly different ($P < 0.05$).

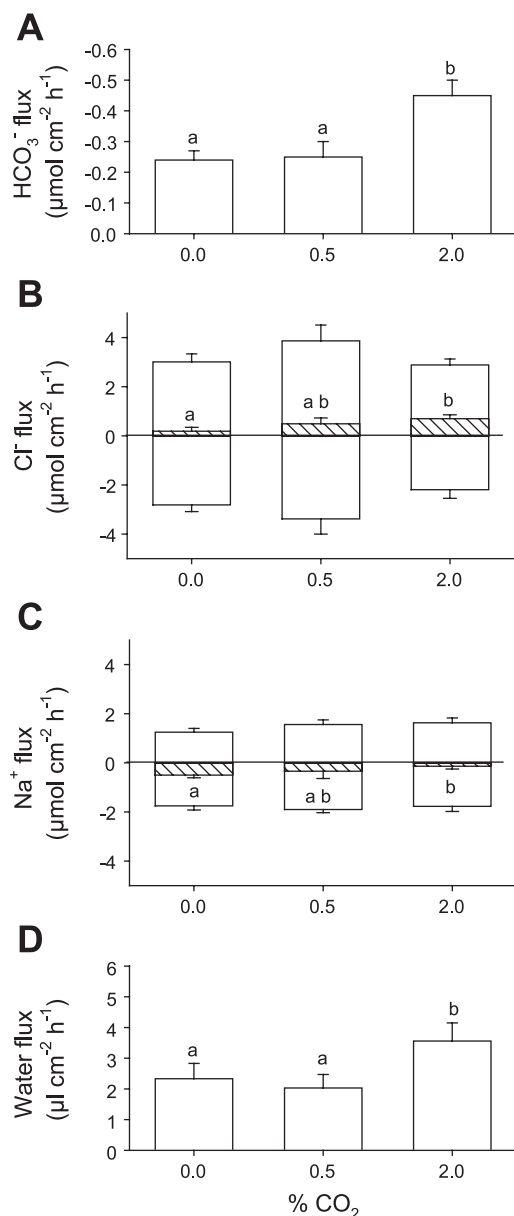


Fig. 5. Net flux of HCO_3^- (A), unidirectional efflux and influx rates (open bars) and net flux rates (hatched bars) of Cl^- (B) and Na^+ (C), and net water movement (D) in isolated intestinal segments from the European flounder in the presence and absence of acetazolamide (10^{-4} M) in both the serosal and mucosal solutions. Experimental animals were injected with acetazolamide in 140 mM NaCl solution 12 h before experimentation to yield an extracellular concentration of 10^{-4} M and acetazolamide (10^{-4} M) was also present in the mucosal and serosal salines throughout the experiments. Control animals were sham-injected with 140 mM NaCl solution. Results are means \pm SE; $n = 15$ and 27 measurements for control and acetazolamide, respectively. Means labeled with different letters are significantly different ($P < 0.05$).

Dixon and Loretz (4). Additional potential basolateral HCO_3^- carriers include the Na^+ - HCO_3^- cotransporter (NBC), as seen in guinea pig and human pancreatic ducts (1, 13), and the electroneutral Na^+ -driven $\text{Cl}^-/\text{HCO}_3^-$ exchanger (NDCBE) identified from human brain (6). However, the previously demonstrated lack of sensitivity of intestinal HCO_3^- secretion to serosal DIDS (10^{-3} M) in the European flounder (8) does not support the involvement of basolateral AE, NBC, or NDCBE,

as these transporters are sensitive to stilbenes (6, 23). Nevertheless, a negative result with DIDS does not conclusively exclude the possible involvement of AE, NBC, and NDCBE, as species-specific differences in DIDS sensitivity do occur (14). The involvement of NDCBE offers an appealing hypothesis because this transporter effectively exchanges NaHCO_3 for HCl (6). Such an exchange would aid not only HCO_3^-

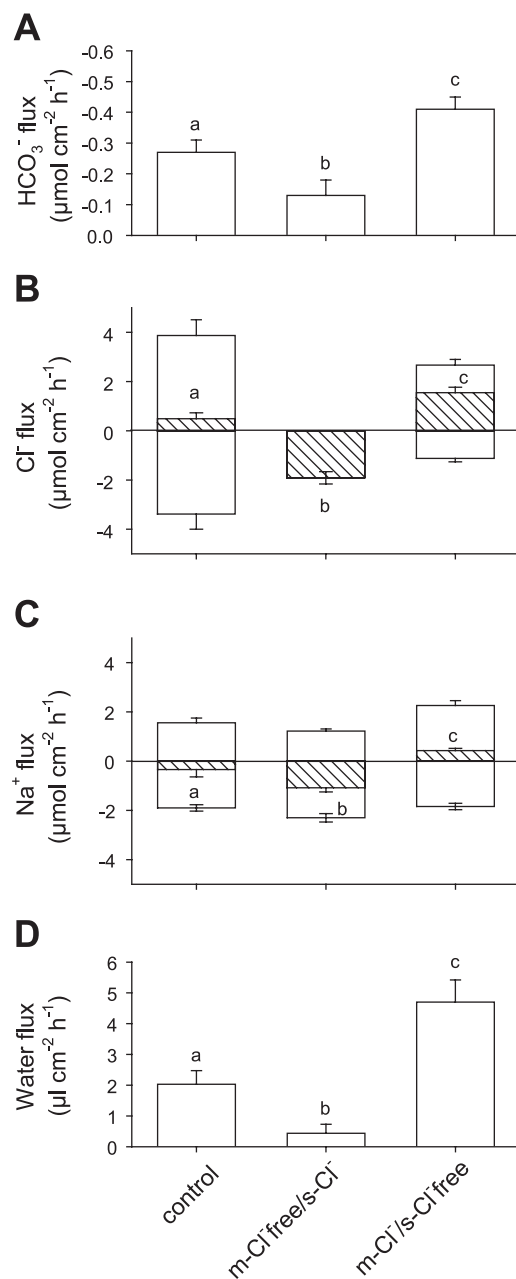


Fig. 6. Net flux of HCO_3^- (A), unidirectional efflux and influx rates (open bars) and net flux rates (hatched bars) of Cl^- (B) and Na^+ (C), and net water movement (D) in isolated intestinal segments from the European flounder in the presence and absence of Cl^- in the mucosal or serosal solutions. m- Cl^- -free/s- Cl^- , absence of Cl^- in the mucosal solution but presence of Cl^- in the serosal solution. m- Cl^- /s- Cl^- -free, absence of Cl^- in the serosal solution but presence of Cl^- in the mucosal solution. Results are means \pm SE; $n = 15$, 20, and 6 measurements in all cases for control, Cl^- -free/ Cl^- , and Cl^- / Cl^- -free conditions, respectively. Means labeled with different letters are significantly different ($P < 0.05$).

Intestinal transepithelial potential (TEP)

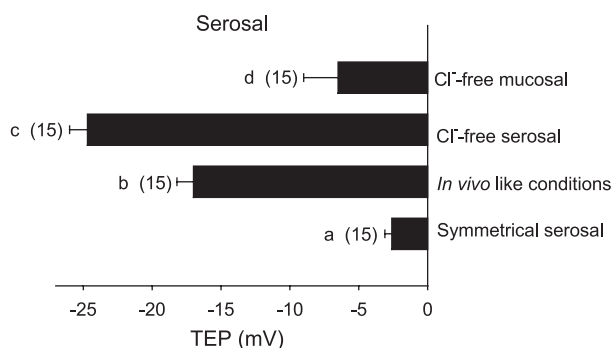


Fig. 7. TEP across the intestinal epithelia of the European flounder under symmetrical (serosal saline on both sides) and asymmetrical [mucosal saline on luminal side, serosal saline on basolateral side (in vivo-like conditions)] conditions in vitro and in the presence and absence of mucosal Cl^- and serosal Cl^- . Results are mean \pm SE; n (no. of measurements) are given in parentheses. Means labeled with different letters are significantly different ($P < 0.05$).

import but also proton extrusion across the basolateral membrane. The latter would prevent reversal of the carbonic anhydrase-mediated CO_2 hydration (10), which seems to be important for HCO_3^- secretion (Figs. 4 and 5, see also Fig. 9). In

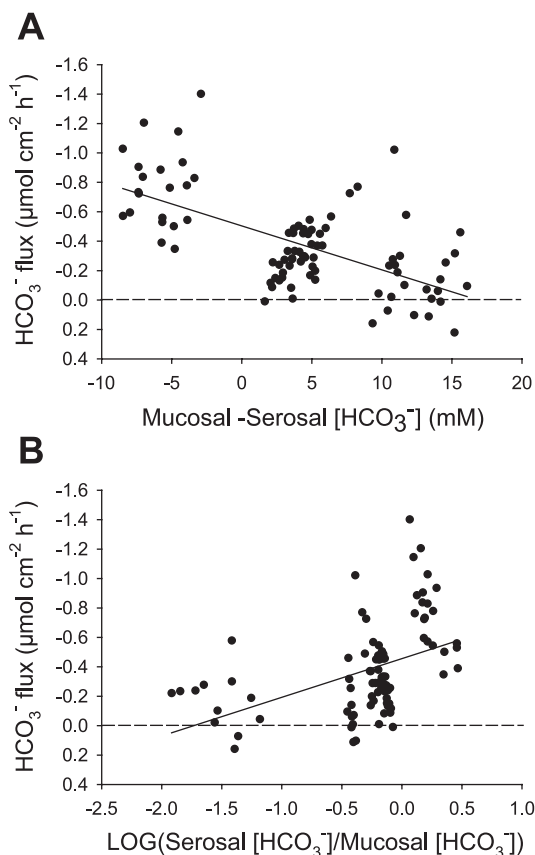


Fig. 8. Individual HCO_3^- secretion rates as a function of transepithelial HCO_3^- gradients across the European flounder intestine. A: secretion rates as a function of the absolute $[\text{HCO}_3^-]$ gradients (mM). B: secretion rates as a function of relative electrochemical HCO_3^- gradients [$\log(\text{serosal } [\text{HCO}_3^-]/\text{mucosal } [\text{HCO}_3^-])$]. Note that HCO_3^- secretion persists against an electrochemical gradient equivalent to an equilibrium potential of -96 mV (i.e., intercept of -1.7), much above the recorded TEP (approximately -16 mV) under identical conditions (Fig. 3).

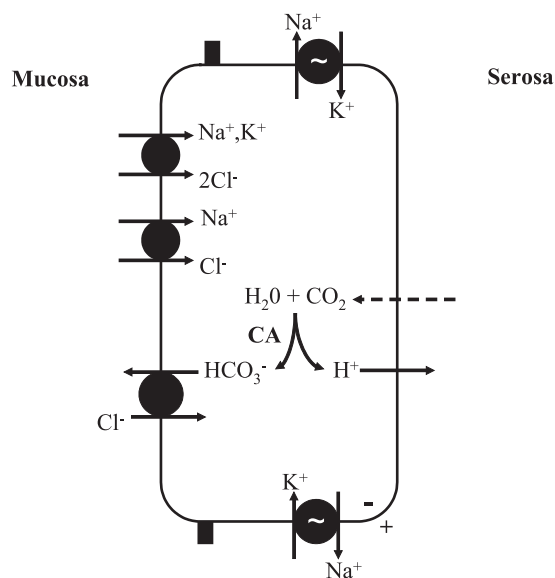


Fig. 9. Transport model of the European flounder intestinal epithelium. Model includes apical $\text{Na}^+\text{-Cl}^-$ and $\text{Na}^+\text{-K}^+\text{-2Cl}^-$ cotransporters and an apical $\text{Cl}^-/\text{HCO}_3^-$ exchanger as well as lateral $\text{Na}^+\text{-K}^+\text{-ATPase}$. Carbonic anhydrase (CA) facilitating CO_2 hydration provides some, but not all, HCO_3^- for the apical $\text{Cl}^-/\text{HCO}_3^-$ exchange process. Both endogenous CO_2 arising from metabolic activity of the intestinal epithelium and CO_2 from the extracellular compartment appear to contribute to HCO_3^- secretion. Protons arising from the CO_2 hydration are extruded across the basolateral membrane, but the mechanism is presently unknown. Possible means of proton extrusion include the proton-ATPase and Na^+/H^+ exchange. Although a proton-ATPase directly could provide energy for the secondary active HCO_3^- secretion, proton extrusion via Na^+/H^+ exchange would rely on the Na^+ gradient established by the $\text{Na}^+\text{-K}^+\text{-ATPase}$.

support of the involvement of NDCBE are previous observations of intestinal HCO_3^- secretion in marine teleosts being dependent on serosal Na^+ (2, 10).

Although the observations of increased HCO_3^- secretion with increased serosal HCO_3^- concentrations strongly suggest transepithelial HCO_3^- transport, it cannot be ruled out that the pH in the serosal fluids, which depends on the HCO_3^- concentration, might have influenced HCO_3^- secretion. The pH in the serosal salines containing 1, 11, and 25 mM HCO_3^- was 6.545 ± 0.021 , 7.810 ± 0.028 , and 8.166 ± 0.071 , respectively. Because the HCO_3^- secretion likely depends on proton extrusion across the basolateral membrane (Fig. 9) and because this extrusion would have occurred against a lower serosal proton concentration in experiments with high serosal HCO_3^- concentrations, elevated basolateral proton extrusion rather than, or in combination with, increased basolateral HCO_3^- import could be responsible for the observed stimulation of HCO_3^- secretion.

A recent report on HCO_3^- secretion in the European flounder did not find evidence for transepithelial HCO_3^- transport (30), which is in contrast to the present study. The discrepancy between these two studies, performed on the same species and using very similar salines but different techniques for measuring HCO_3^- secretion, could perhaps be explained by the different temperatures at which these studies were conducted. The present study was conducted at a slightly lower temperature (12°C compared with 14°C), and it seems likely that the higher temperature in the previous study (30) would increase epithelial metabolic rate and thereby CO_2 production, reducing the

need for basolateral HCO_3^- import to sustain luminal secretion. An additional possible explanation for the discrepancy is that, whereas the serosal pH varied with the serosal HCO_3^- concentration in the present study, the previous study was conducted in the presence and absence of serosal HCO_3^- but at constant pH (30). The reduced pH in serosal salines containing 1 mM HCO_3^- in the present study may have impaired proton secretion and thus HCO_3^- secretion, whereas this would not have been the case in the previous study, which used HEPES buffering in the HCO_3^- -free serosal saline.

It seems that elevated serosal CO_2 (2%) may fuel CO_2 hydration, which provides HCO_3^- for luminal secretion (Fig. 4). Elevating serosal CO_2 from 0.5 to 2.0% resulted in a slightly increased serosal HCO_3^- concentration (measured values at start of flux period of 9.62 ± 0.10 and 10.27 ± 0.05 , respectively) and a change in pH from 7.77 to 7.22 at the beginning of the flux period. Reduced serosal pH cannot explain the increased HCO_3^- secretion seen in these experiments, as elevated serosal proton concentrations would lead to reduced basolateral proton extrusion and thus reduced apical HCO_3^- secretion (Fig. 9). Furthermore, the slight increase in serosal HCO_3^- concentration is not sufficient to explain the twofold elevation in HCO_3^- secretion rate, which must therefore be the result of elevated CO_2 . However, it is also clear that endogenous CO_2 production is sufficient to provide most of the CO_2 for hydration under physiological conditions (0.5% CO_2) because removal of this serosal CO_2 does not lead to reduced HCO_3^- secretion. These latter findings are in agreement with recent studies on the European flounder, which concluded that endogenous CO_2 was fueling the HCO_3^- secretion (30). Previous estimates of the metabolic rate of the intestinal tissue of a marine teleost in the context of HCO_3^- secretion suggested that endogenous CO_2 production rates may be insufficient in sustaining the observed HCO_3^- secretion metabolic rate (10). However, it should be noted that these estimates were not based on actual measurements of intestinal epithelium metabolic rate. Because the metabolic rate of the intestinal epithelium can be expected to be high, compared with whole animal metabolic rate, which formed the basis for the above estimates, these estimates might have underestimated the potential contribution of endogenous metabolic CO_2 .

Carbonic anhydrase appears to facilitate CO_2 hydration, which fuels HCO_3^- secretion in that application of the carbonic anhydrase inhibitor acetazolamide led to a reduction in HCO_3^- secretion rate (Fig. 7). This observation is in agreement with a previous report of reduced intestinal HCO_3^- secretion rate caused by acetazolamide treatment in seawater-acclimated rainbow trout (29). Neither in the present study nor in the study performed on rainbow trout did inhibition of carbonic anhydrase completely abolish HCO_3^- secretion, suggesting that noncatalyzed CO_2 hydration is sufficient to support part of the intestinal HCO_3^- secretion.

Interactions between HCO_3^- secretion and Cl^- . Cl^- -free mucosal saline greatly reduced but did not completely abolish HCO_3^- secretion (Fig. 6), which is in agreement with previous reports from several marine teleost fish (2, 10, 29). Measurements of Cl^- in the mucosal “ Cl^- -free” saline revealed an average of 3.5 mM Cl^- and 20.7 mM Cl^- in samples obtained at the beginning and at the end of the flux periods, respectively. Low levels of Cl^- in the Cl^- -free saline, presumably coming from incomplete rinsing of the intestinal lumen at the begin-

ning and from serosal-to-mucosal Cl^- diffusion during the experiments, is perhaps the reason for the remaining HCO_3^- secretion, mediated by apical anion exchange, observed under these conditions. A slight net Na^+ loss seen in control preparations was greatly increased under Cl^- -free mucosal conditions, clearly showing the involvement of $\text{Na}^+\text{-Cl}^-$ and/or $\text{Na}^+\text{-K}^+\text{-2Cl}^-$ cotransporters in intestinal NaCl absorption.

Removal of serosal Cl^- enhanced HCO_3^- secretion (Fig. 6), which is in contrast to previous studies performed on the Pacific sanddab, where removal of serosal Cl^- had no effect on HCO_3^- secretion (10). The reason for this discrepancy is unknown, but the difference likely reflects that different transport mechanisms are involved in HCO_3^- secretion in these two species. Removal of serosal Cl^- effectively reverses the electrochemical gradient for Cl^- across the intestinal epithelium and resulted in a more negative TEP (Fig. 7), which may have contributed to the enhanced HCO_3^- secretion. In the European flounder, serosal Cl^- removal not only increased the net absorption of Cl^- , and thereby the HCO_3^- secretion, driven by apical anion exchange but also reversed the net Na^+ loss seen in control preparations to a slight net Na^+ uptake (Fig. 6), again showing the involvement of NaCl cotransporters.

Contribution of $\text{Cl}^-/\text{HCO}_3^-$ exchange to Cl^- and water transport. All control preparations with the exception of those displayed in Fig. 2 exhibited significant water absorption (overall mean of $2.12 \pm 0.30 \mu\text{l}\cdot\text{cm}^{-2}\cdot\text{h}^{-1}$, $n = 99$). The reason for the lack of water absorption in the control preparations of Fig. 2 is unknown. The present data suggest that anion exchange may contribute significantly to Cl^- and water absorption across the intestinal epithelium. Elevated HCO_3^- secretion caused by increased serosal HCO_3^- concentration, Cl^- -free serosal salines, and increased CO_2 results in increased net Cl^- and fluid absorption (Figs. 1, 4, and 6), although this was not statistically significant in the case of fluid absorption during exposure to elevated serosal HCO_3^- . Reduction of HCO_3^- secretion by increased mucosal-serosal HCO_3^- gradients (Fig. 2) or exposure to the carbonic anhydrase inhibitor acetazolamide, however, did not result in significant reduction of net Cl^- and fluid absorption. Removal of mucosal Cl^- , depleting both the anion exchange process and the $\text{Na}^+\text{-Cl}^-$ and/or $\text{Na}^+\text{-K}^+\text{-2Cl}^-$ cotransport systems, however, resulted in reduced HCO_3^- secretion and fluid absorption as well as increased net Na^+ loss. Conversely, removal of serosal Cl^- stimulated HCO_3^- secretion as well as net Na^+ and fluid absorption. It thus appears that two parallel systems exist for Cl^- and fluid absorption across the marine teleost intestine, one being the traditionally accepted $\text{Na}^+\text{-Cl}^-$ and/or $\text{Na}^+\text{-K}^+\text{-2Cl}^-$ cotransport pathway and the other being an anion-exchange-mediated system. From the present study, it appears that the relative importance of these two systems may depend on luminal chemistry and perhaps other parameters. In the case of reduced HCO_3^- secretion, Cl^- and fluid absorption still persist, presumably mediated by the $\text{Na}^+\text{-Cl}^-$ and/or $\text{Na}^+\text{-K}^+\text{-2Cl}^-$ system. However, in the case of stimulated HCO_3^- secretion, it appears that both Cl^- and fluid absorption are also stimulated, suggesting an important role of this system in marine teleost osmoregulation.

It is not possible from the present data to accurately separate the relative contributions of these two systems. It should be noted, however, that the HCO_3^- secretion rates observed in the isolated intestinal segments are lower than the corresponding

rates observed in vivo and that stimulated HCO_3^- secretion rates in the present study (approaching those seen in vivo) stimulate Cl^- and fluid absorption rates. This may suggest that the anion exchange is relatively more important under in vivo conditions. Indeed, an in situ intestinal perfusion study performed on the lemon sole, *Parophrys vetulus*, revealed Cl^- absorption rates twice as high as the corresponding rates for Na^+ , with the difference accounted for by HCO_3^- secretion rates. This was interpreted to mean that the $\text{Cl}^-/\text{HCO}_3^-$ exchange system accounted for ~50% of the total Cl^- absorption (7). Furthermore, when Na^+ uptake was completely inhibited by treatment with silver, substantial Cl^- absorption persisted and matched perfectly with HCO_3^- secretion, and no reduction in fluid absorption was observed (7). It thus appears that intestinal anion exchange may play a quantitatively important role in Cl^- and fluid absorption across marine teleost intestinal epithelia.

The mechanism(s) of water transport continues to be a controversial topic, but there seems to be general consensus that fluid movement is driven by NaCl transport and that the absorbate is isotonic (16, 17). In the present study, in almost all cases, significant water absorption was observed in the absence of net Na^+ absorption, which contrasts with this general view. Water absorption occurred despite no transepithelial difference in osmotic pressure. It is clear, however, that fluid absorption across the European flounder intestine is linked to active net Cl^- uptake (Figs. 1, 4, and 6). Cl^- absorption must be associated with accompanying cation absorption or anion secretion to maintain charge balance in the absorbed fluid. Considering all control measurements in the present study, mean net Cl^- absorption was $0.58 \pm 0.04 \mu\text{mol} \cdot \text{cm}^{-2} \cdot \text{h}^{-1}$ and net HCO_3^- secretion was $0.28 \pm 0.02 \mu\text{mol} \cdot \text{cm}^{-2} \cdot \text{h}^{-1}$ ($n = 99$). This suggests that $0.3 \mu\text{eq}$ of cation $\text{cm}^{-2} \cdot \text{h}^{-1}$ (different from Na^+) must have been absorbed in conjunction with the absorbed Cl^- . K^+ , Ca^{2+} , and Mg^{2+} are possible candidates, but the net transport rates of these ions were not measured in the present study. The observed active HCO_3^- secretion must be associated with proton extrusion to prevent reversal of the (carbonic anhydrase-mediated) CO_2 hydration reaction. It has been argued that this proton extrusion must occur predominantly across the basolateral membrane because the intestinal epithelium exhibits net base secretion (10) (Fig. 9). Basolateral proton extrusion may account for part of the “missing cation” required for charge balance, which would result in an acidic absorbate. The mechanism of basolateral H^+ extrusion is presently unknown and offers an exciting area for future studies.

Perspectives

In conclusion, the intestinal epithelium of the European flounder is capable of secondary active HCO_3^- secretion, and this may be a general phenomenon of marine teleost fish. This secretion occurs via anion exchange, contributes significantly to Cl^- absorption, and provides an explanation for fluid absorption in the absence of net Na^+ absorption. The marine teleost intestine offers an interesting comparison to other fluid-absorbing epithelia, including the mammalian duodenum and the vertebrate gall bladder and renal tubules, and is an easily

accessible organ of practical size for experimentation. Furthermore, the ability of the intestinal epithelium to perform secondary active HCO_3^- secretion, yielding luminal concentrations in excess of 100 mM, greatly resembles that of the ducts of the exocrine pancreas, an organ which is far from fully understood (22). The marine teleost intestine may thus be an interesting model for studies of active epithelial HCO_3^- secretion and may offer insight into the mechanisms of this transport system not only in fish intestines but also in other organ systems of higher vertebrates.

GRANTS

This work was supported by a National Science Foundation Grant (0416440) to M. Grosell and a National Sciences and Engineering Research Council discovery grant to C. M. Wood. C. M. Wood is supported by the Canadian Research Chair Program.

REFERENCES

1. Abuladze N, Lee I, Newman D, Hwang J, and Boorer K. Molecular cloning, chromosomal localization, tissue distribution, functional expression of the human pancreatic sodium bicarbonate co-transporter. *J Biol Chem* 273: 17689–17695, 1998.
2. Ando M and Subramanyam MVV. Bicarbonate transport systems in the intestine of the seawater eel. *J Exp Biol* 150: 381–394, 1990.
3. Boutilier RG, Heming TA, and Iwama GK. Appendix: Physicochemical parameters for use in fish respiratory physiology. *Fish Physiol* X: 403–430, 1984.
4. Dixon JM and Loretz CA. Luminal alkalization in the intestine of the goby. *J Comp Physiol [B]* 156: 803–811, 1986.
5. Field M, Smith PL, and Bolton JE. Ion transport across the isolated intestinal mucosa of the winter flounder *Pseudopleuronectes americanus*. II. Effects of cyclic AMP. *J Membr Biol* 53: 157–163, 1980.
6. Grichtchenko II, Choi I, Zhong X, Bray-Ward P, Russell JM, and Boron WF. Cloning, characterization, and chromosomal mapping of a human electroneutral Na^+ -driven $\text{Cl}^-/\text{HCO}_3^-$ exchanger. *J Biol Chem* 276: 8358–8363, 2001.
7. Grosell M, De Boeck G, Johannsson O, and Wood CM. The effects of silver on intestinal ion and acid-base regulation in the marine teleost fish, *Papophrys vetulus*. *Comp Biochem Physiol C* 124: 259–270, 1999.
8. Grosell M and Jensen FB. NO_2^- uptake and HCO_3^- excretion in the intestine of the European flounder (*Platichthys flesus*). *J Exp Biol* 202: 2103–2110, 1999.
9. Grosell M and Jensen FB. Uptake and effects of nitrite in the marine teleost fish *Platichthys flesus*. *Aquat Toxicol (Amst)* 50: 97–107, 2000.
10. Grosell M, Laliberte CN, Wood S, Jensen FB, and Wood CM. Intestinal HCO_3^- secretion in marine teleost fish: evidence for an apical rather than a basolateral $\text{Cl}^-/\text{HCO}_3^-$ exchanger. *Fish Physiol Biochem* 24: 81–95, 2001.
11. Grosell M, O'Donnell MJ, and Wood CM. Hepatic versus gallbladder bile composition: in vivo transport physiology of the gallbladder in rainbow trout. *Am J Physiol Regul Integr Comp Physiol* 278: R1674–R1684, 2000.
12. Halm DR, Krasny EJ, and Frizzell RA. Electrophysiology of flounder intestinal mucosa. II. Relation of the electrical potential profile to coupled NaCl absorption. *J Gen Physiol* 85: 865–883, 1985.
13. Ishiguro H, Steward MC, Lindsay ARG, and Case RM. Accumulation of intracellular HCO_3^- by $\text{Na}^+/\text{HCO}_3^-$ cotransport in interlobular ducts from guinea-pig pancreas. *J Physiol* 495: 169–178, 1996.
14. Jensen FB and Brahm J. Kinetics of chloride transport across fish red blood cell membranes. *J Exp Biol* 198: 2237–2244, 1995.
15. Karnaky KJ. Osmotic and ionic regulation. In: *The Physiology of Fishes*, edited by Evans DH. Boca Raton, FL: CRC, 1998, p. 157–176.
16. Larsen EH. Role of lateral intercellular space and sodium recirculation for isotonic transport in leaky epithelia. *Rev Physiol Biochem Pharmacol* 141: 153–212, 2000.
17. Larsen EH, Sørensen JB, and Sørensen JN. Analysis of the sodium recirculation theory of solute-coupled water transport in small intestine. *J Physiol* 542: 33–50, 2002.

18. **Loretz CA.** Electrophysiology of ion transport in the teleost intestinal cells. Cellular and molecular approaches to fish ionic regulation. *Fish Physiol* 14: 25–56, 1995.
19. **Mackay WC and Lahlou B.** Relationships between Na^+ and Cl^- fluxes in the intestine of the European flounder, *Platichthys flesus*. Epithelial transport in lower vertebrates. In: *Epithelial Transport in Lower Vertebrates*, edited by Lahlou B. Cambridge, UK: Cambridge Univ. Press, 1980, 151–162.
20. **Marvao P, Emilio MG, Ferreira KG, Fernandes PL, and Ferreira HG.** Ion-transport in the intestine of *Anguilla anguilla*—gradients and translocators. *J Exp Biol* 193: 97–117, 1994.
22. **Novak I.** Keeping up with bicarbonate. *J Physiol* 528: 235–235, 2000.
23. **Romeo MF and Boron WF.** Electrogenic $\text{Na}^+/\text{HCO}_3^-$ cotransporters: cloning and physiology. *Annu Rev Physiol* 61: 699–723, 1999.
24. **Shehadeh ZH and Gordon MS.** The role of the intestine in salinity adaptation of the rainbow trout, *Salmo gairdneri*. *Comp Biochem Physiol A* 30: 397–418, 1969.
25. **Smith HW.** The absorption and excretion of water and salts by marine teleosts. *Am J Physiol* 93: 480–505, 1930.
26. **Walsh PJ, Blackwelder P, Gill KA, Danulat E, and Mommsen TP.** Carbonate deposits in marine fish intestines: a new source of biomineralization. *Limnol Oceanogr* 36: 1227–1232, 1991.
27. **Walton Smith FG.** *CRC Handbook of Marine Science*. Cleveland, OH: CRC, 1931, vol 1.
28. **Wilson RW.** A novel role for the gut of seawater teleosts in acid-base balance. In: *Regulation of Acid-Base Status in Animals and Plants. SEB Seminar Series*. Cambridge, UK: Cambridge Univ. Press, 1999, vol. 68, p. 257–274.
29. **Wilson RW, Gilmour K, Henry R, and Wood C.** Intestinal base excretion in the seawater-adapted rainbow trout: a role in acid-base balance? *J Exp Biol* 199: 2331–2343, 1996.
30. **Wilson RW and Grosell M.** Intestinal bicarbonate secretion in marine teleost fish—source of bicarbonate, pH sensitivity, and consequence for whole animal acid-base and divalent cation homeostasis. *Biochim Biophys Acta* 1618: 163–174, 2003.
31. **Wilson RW, Wilson JM, and Grosell M.** Intestinal bicarbonate secretion by marine teleost fish—why and how? *Biochim Biophys Acta* 1566: 182–193, 2002.

